Distribution of size fractionated dissolved iron in the Canary Basin

Simon J. Ussher [a],[*], Eric P. Achterberg [b], Géraldine Sarthou [c], Patrick Laan [d], Hein J.W. de Baar [d], Paul J. Worsfold [a]

[a] School of Geography, Earth and Environmental Sciences, University of Plymouth, Plymouth PL4 8AA, UK
[b] National Oceanography Centre, University of Southampton, SO14 3ZH, UK
[c] LEMAR/UMR CNRS 6539/IUEM, Technopole Brest Iroise, F-29280 Plouzané, France
[d] Royal Netherlands Institute for Sea Research (Royal NIOZ), Postbus 59, 1790 AB Den Burg – Texel, The Netherlands

ARTICLE INFO

ABSTRACT

The distribution of size fractionated dissolved iron (DFe, <0.2 μm) species was determined in the upper water column (0–150 m) of the Canary Basin (25–32°N and 18–24°W) on a research cruise in October 2002. A DFe concentration gradient resulting from a decrease in both soluble iron (SFe, <0.02 μm) and colloidal iron (CFe, 0.02–0.2 μm) was shown to extend from the coast of North West Africa into the oligotrophic gyre (varying from ∼1 nM in the shelf region to 0.15 nM in the most off shore waters). At the time of this study, the dominant dissolved Fe input to the region was deduced to be the advection of shelf and upwelled waters rather than Saharan dust deposition.

SFe and CFe fractions had mean concentrations ($\pm$ one standard deviation) of 0.25 $\pm$ 0.11 and 0.21 $\pm$ 0.16 nM, respectively ($n = 58$). Colloidal iron formed a highly variable fraction of DFe (ca. 0–80%, mean of 42%) in the region but was less variable in the low iron, oligotrophic intermediate waters (0.18 $\pm$ 0.06 nM, 31.7°N, 22.0°W, 0–1300 m depth). The high variability found at the most productive near-shelf stations was driven by biological processing and mixing of different water masses. In contrast, less variability between SFe and CFe at the remote off shore stations suggested that vertical variations in the water column were controlled more by chemical partitioning and vertical particle fluxes with evidence of preferential biological uptake and/or removal of SFe in the most remote surface waters.

1. Introduction

Iron plays a major role in the regulation of primary production in the oceans (Falkowski et al., 1998) and its biogeochemistry is dynamic in comparison with other trace metals (e.g. Zn, Cd) due to its low solubility and relatively short residence time in seawater (Bruland et al., 1994; Landing and Bruland, 1987). The growth of phytoplankton in remote ocean regions can be limited due to low iron concentrations (Martin and Fitzwater, 1988). Evidence for iron-limitation has been reported following *in situ* iron fertilization experiments in the high nutrient low chlorophyll (HNLC) regions of the Southern and Pacific Oceans (Boyd et al., 2000; Coale et al., 2004, 1996; Martin et al., 1994; Tsuda et al., 2003).

The transport of iron to the surface ocean occurs via several mechanisms, including fluvial inputs and deepwater entrainment (de Baar and de Jong, 2001). Strong evidence that coastal upwelling and mesoscale eddies are a major pathway of iron transport to the

open ocean has been reported (Chase et al., 2005; Johnson et al., 2005). A significant fraction of DFe advected from shelf regions may originate from the release of iron following diagenetic reduction processes in shelf sediments (Elrod et al., 2004), and advection of degraded organic matter and communities of micro-organisms in productive regions may also contribute to Fe transport. Horizontal transport of dissolved and particulate iron has been shown to have an important impact on adjacent iron limited regions near the Crozet and Kerguelen Islands in the Southern Ocean (Planquette et al., 2007, 2009; Blain et al., 2008). In addition, transport of Fe rich particles to the subarctic North Pacific has been traced to continental margins (Lam et al., 2006).

Atmospheric deposition provides an additional significant Fe input to surface waters, making this an important source for remote open ocean ecosystems (Duce and Tindale, 1991; Jickells et al., 2005). The residence time of atmospherically derived dissolved iron (DFe, <0.2 μm) in the sub-tropical surface Atlantic Ocean has been estimated to be in the order of weeks (9–54 days) (Sarthou et al., 2003) to months (60–300 days) (de Baar and de Jong, 2001; Jickells, 1999). Consequently, the seasonal and inter-annual variation of aerosol fluxes can cause large changes (0.1–2.0 nM) in

* Corresponding author. Tel.: +44 1752 584566.
  E-mail address: sussher@plymouth.ac.uk (S.J. Ussher).

surface DFe concentrations in the mixed layer of oceanic waters, which in turn, will cause changes to the resident microbial populations (Sedwick et al., 2005).

The amount of DFe delivered by aerosol deposition of particulate iron will also vary depending on the dissolvable fraction of Fe in deposited aerosols. A recent survey of the solubility of Fe from aerosols collected in different Atlantic provinces showed considerable variation (1.4–54%), attributed to the aerosol source as well as their physical and chemical composition (Baker et al., 2006). A similar solubility range of Fe from aerosols (0–53%) was also reported for de-ionised water leaches of Pacific aerosols (Buck et al., 2006). Atlantic aerosol samples identified as Saharan dusts were found to have comparatively low solubility with a median of 1.7% (Baker et al., 2006). Hence, a high percentage (>90%) of aerosol Fe of Saharan origin deposited over high dust impacted regions, such as the Canary Basin, will be unavailable to phytoplankton as it is rapidly removed from the surface waters by sinking.

Following dissolution from aerosol dust particles, the vertical distribution of DFe within the open ocean water column is largely controlled by the rates of scavenging and biological uptake, which depend on the speciation of iron. Workers have shown that >99% of DFe is strongly complexed by Fe binding ligands in seawater (Powell and Donat, 2001; Rue and Bruland, 1995; van den Berg, 1995), and the nature of the Fe binding ligands will influence the biogeochemical cycling of iron (Ussher et al., 2004).

DFe can be operationally divided into 'colloidal' and 'soluble' phases by the pore size of the filtration method used. Laboratory iron solubility studies in seawater have shown that ambient soluble Fe (SFe) concentrations generally exceed the Fe solubility of a purely inorganic matrix (defined as Fe passing through a 0.02 or 0.025 µm pore size filter) due to the presence of strong Fe binding ligands (Byrne et al., 2000; Kuma et al., 1998, 1996; Liu and Millero, 1999, 2002). Furthermore, variations in Fe solubility (0.1–1.6 nM) in seawater from different depths have been observed following saturation with radio-labeled Fe (Kuma et al., 1996; Tani et al., 2003). These experiments showed that the SFe concentrations in seawater varied significantly according to the composition and physico-chemical conditions of the seawater.

In the North Atlantic Ocean, the colloidal Fe fraction (defined as 0.02–0.4 µm) has been reported as highly variable, ranging between 0% and 95% in surface waters and 30–70% in deep waters (>3000 m) (Cullen et al., 2006; Wu et al., 2001). Bergquist et al. (2007) concluded that the major variation in DFe in Atlantic surface waters was due to changes in CFe rather than SFe, as the latter remained relatively constant. This lead to the hypothesis that the residence times of different Fe species are likely to vary depending on their bioavailability and scavenging efficiency.

There have been relatively few reports of the variability of soluble Fe concentrations in oceanic provinces that receive high inputs of DFe. For this study, the Canary Basin was chosen as a suitable study area for examining Fe size speciation as the Fe fluxes to surface waters are high and variable. The dominant winds in the Canary Basin are the north-easterly trade winds, which cause significant upwelling along the North West African coast, coastal filaments and cyclonic eddies that cause offshore export of nutrients and organic matter (Barton, 1998; Pelegrí et al., 2005). Furthermore, the region is situated under the seasonal transport path of the Saharan dust plume which transports large quantities of Fe in dust originating from arid regions in North Africa across the North Atlantic Ocean (Duce and Tindale, 1991). It has been estimated that over a million tonnes of dust (>40,000 tonnes of Fe) are deposited over the Canary Islands region every year. However, the dust deposition in this region is episodic, occurring in pulses of 3–8 days and is highest during winter and summer (42% and 29% of the annual deposition occurring between January–March and July–September, respectively) (Torres-Padron et al., 2002). The high aerosol deposition in this region causes elevated downward fluxes of particulate iron in the water column, compared with other regions of the Northeast Atlantic (Kremling and Streu, 1993; Kuss and Kremling, 1999a,b). Reported average particulate iron fluxes in the water column of the Canary Basin were around 4 times higher than those observed at stations between 30 and 55°N (Kuss and Kremling, 1999a).

In this paper we report the results from a study of dissolved iron size speciation in surface waters (0–150 m) of the Canary Basin. The specific aims of the work were to (i) determine the spatial distribution of size fractionated iron species in this region and (ii) examine the variation in the colloidal and soluble Fe in this region in relation to vertical and lateral transport pathways and biological processing.

2. Methods

Surface water (5 m), shallow cast (0–150 m) and oligotrophic intermediate/deep water samples (150–5000 m) were collected on the RV Pelagia (Royal NIOZ, The Netherlands) along a defined grid (25–32°N and 18–24°W) west of the Canary Islands in the Eastern North Atlantic Ocean (Fig. 1). The 'IRONAGES III' cruise took place in autumn (2nd–31st October) 2002. All casts (8–23) were undertaken in the morning between 08:30 and 09:30 h (local time), except for casts 13 and 15, which took place at 13:30 h and 15:00 h, respectively. Cast samples for DFe species were taken from precleaned, PTFE coated GoFlo bottles (General Oceanics™) which were deployed on a Kevlar line (de Jong et al., 1998). After recovery,
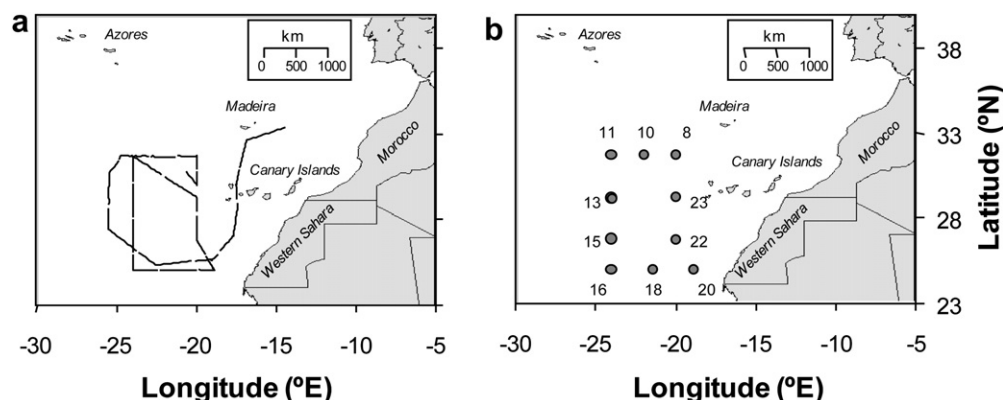

Fig. 1. 'Iron from above' study area (October 2002), showing (a) surface cruise track in the study area and (b) CTD vertical profile stations.

the bottles were immediately mounted in a laminar flow cabinet in a clean container. Underway surface water sampling was conducted between stations whilst the ship was steaming ($\sim$12 knots) using a trace metal clean towed fish deployed 5 m from the starboard side of the ship (Croot and Laan, 2002). The towed fish was connected by PTFE tubing to a PTFE bellows pump (Almatec™ A-15), which provided a flow rate of approximately 3 L min^{-1}. The pump was driven by a compressor (Jun-Air™, model 600-4B) operating at a pressure of 1.5–2 bar.

2.1. Trace metal sample processing

All sample handling was conducted using trace metal clean protocols in a class 100 laminar flow hood inside a clean laboratory container. Samples for DFe were filtered through Sartobran cartridges (0.2 μm pore size, cellulose acetate membrane, Sartorius™), either in-line from the surface pump supply or using filtered nitrogen overpressure on the GoFlo bottles. Discrete cast samples for DFe were collected in 250 mL, acid washed, low density polyethylene (LDPE) bottles (Nalgene™) which were previously stored, filled with acidified high purity water (18.2 MΩ cm^{-1}, Elga™, 0.01 M quartz distilled HCl, VWR™). Cast sample filtration was completed within 1.5 h after collection and the samples were then acidified (pH 1.9, quartz distilled HCl) and stored for laboratory analysis.

Sub-samples for soluble iron (SFe, <0.02 μm) were collected at cast stations following in-line filtration through 0.02 μm pore size, sealed syringe filters (25 mm diameter, Anotop™, Whatman). Prior to use, these filters were cleaned in-line according to the method of Wu et al. (2001) by washing each filter with 30 mL of 0.1% HCl followed by 60 mL of high purity water and 60 mL of sample. Instead of syringes, solution and samples were delivered to the filter via PTFE tubing (0.8 mm ID, Fisher) and pump tubing (PVC, Elkay) attached to a peristaltic pump (Minipuls 3, Gilson) set at 1 mL min^{-1}. For soluble iron determinations, samples were stored and analysed using the same method as for DFe, stated below. Colloidal iron (CFe, 0.02–0.2 μm) was determined by calculating the difference between the two filtered fractions (i.e. CFe = DFe – SFe) and therefore was an operationally defined fraction that excluded colloids outside of this size range.

2.2. Analytical methods

The acidified samples were stored in the dark for 4–6 months before analysis and all analyses and subsequent sample handling were conducted in an accredited (ISO9001:2000) shore based clean room. DFe and SFe were determined using FI-CL using luminol reagent with no added oxidant following a 12 h sulphite reduction step (Bowie et al., 1998). All Fe data reported were the mean values of 4 replicate analyses on a single sample (where peak height was measured). It should be noted that a thorough interpretation of 'shipboard' DFe (using an acidification time of >24 h and different FI-CL analyser) and dissolved aluminium (DAl) are reported elsewhere (Kramer et al., 2004; Sarthou et al., 2007).

The accuracy of the method used here was tested by the determination of DFe in an IRONAGES reference standard (bottle no. 233, Atlantic surface water (Bowie et al., 2006)). The concentration determined was 0.55 $\pm$ 0.05 nM, which was within the standard deviation of the consensus concentration of a community-wide separate bottle intercomparison (0.59 $\pm$ 0.21 nM). SAFe reference seawaters (bottle numbers S530 and D160, North Pacific seawater (Johnson et al., 2007)) were also analysed and DFe concentrations were 0.20 $\pm$ 0.02 nM and 0.91 $\pm$ 0.03 nM for the surface and deep samples, respectively. There was excellent agreement between the deep sample concentration and the

community consensus concentration (0.91 $\pm$ 0.17 nM), whereas a positive bias ($\sim$0.1 nM) was found for the DFe concentration of the surface sample compared to the community consensus concentration (0.097 $\pm$ 0.043 nM).

More recently, the DFe analytical method was validated by analysis of five IRONAGES reference standards and the results for the same sub-samples were compared to those obtained by co-precipitation followed by isotope dilution inductively coupled plasma mass spectrometry (ICP-MS) (Bowie et al., 2007). The mean concentration of the 5 samples was 0.549 $\pm$ 0.044 nM, when analysed by FI-CL, and 0.553 $\pm$ 0.050 nM, when analysed by ICP-MS. The mean concentration of the 5 bottles showed no significant difference ($P = 0.05$) between methods.

2.3. Supporting oceanographic data

Supporting data were provided by workers from the Royal Netherlands Institute for Sea Research (Royal NIOZ) and included physical data from underway and CTD systems, chlorophyll a (Chl a) and nutrient data. Samples for nutrients (nitrate, nitrite and phosphate) were collected in high-density polyethylene sample bottles, filtered through 0.2 μm filter cartridges (Sartrobran-300, Sartorius) and stored in the dark at 4 °C in a polyethylene cup. Nitrate, nitrite and phosphate were then determined spectrophotometrically using segmented flow analysis (Grashoff, 1983) on a Technicon TrAAcs 800 AutoAnalyzer within 8 h of sample collection. Samples for Chl a were collected on a GF/F filter, after filtration of $\sim$1 L of seawater. The filters were stored at −80 °C and analysed by HPLC according to Veldhuis and Kraay (2004). Discrete water samples were taken for direct analysis of the phytoplankton community using a Coulter XL-MCL flow cytometer (Veldhuis and Kraay, 2004).

3. Results and discussion

3.1. Hydrography and aerosol fluxes

The upper water column (0–150 m) in the study area was stratified during the cruise period showing enhanced temperatures (18–26 °C) and salinities (36.0–37.5), typical of North Atlantic Surface Water (NASW). Mixed layer depths (MLDs) varied between 30 and 60 m, with the shallowest MLDs (<50 m) observed in the north (casts 8, 10 and 11) and south east of the sampling grid (cast 20). The surface currents in the region were dominated by the south west moving Canary Current which flows approximately parallel to the North West African coast until the south west tip of Western Sahara at ca. 20°N, where it deflects offshore. As the closest sources of iron to the surface waters in this region were the adjacent land masses of Portugal and North West Africa, the physico-chemical underway/surface water data were plotted against the perpendicular distance between each sample station and the North West African coast (estimated as a line from 34°N, 8°W to 25°N, 16°W) (Fig. 2). The underway temperature and salinity data for the surface waters (5 m depth) of the study area plotted versus the distance from the coast are shown in Fig. 2(a, b). Surface water temperature ranged from a minimum between 22 and 23 °C near Madeira (30–34°N, 15–17.5°W), to a maximum >25 °C in the south west of the study area (25–28°N, 21–25°W). The highest salinity waters (<37.8) were located in the western side of the grid (23–26°W), whereas the lowest salinity waters (<37) were found <600 km from the coast which was indicative of mixing of NASW with waters of lower salinity near the continental margin.

The *in situ* aerosol fluxes of soluble iron to the Canary Basin were estimated from measured air concentrations for 12 time periods during the cruise and details of the methods and data can be found
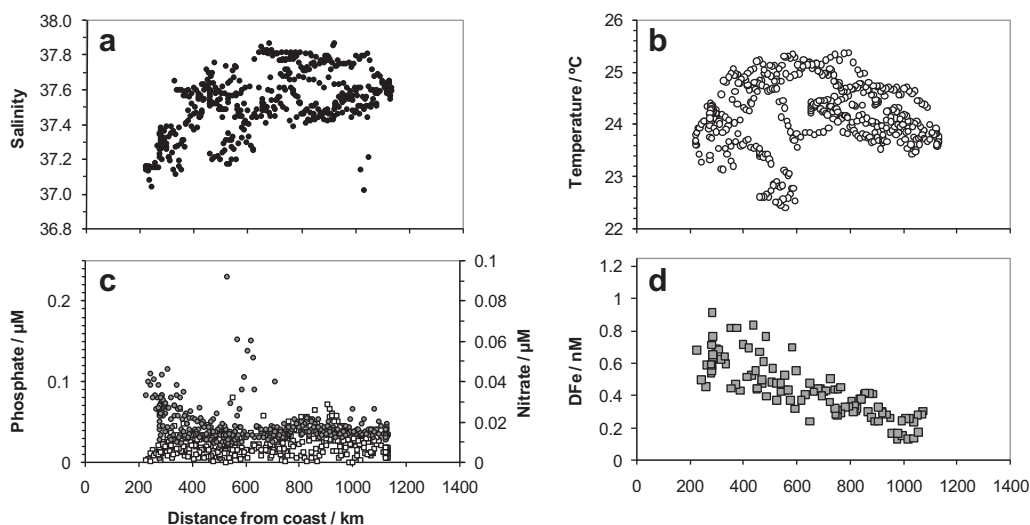
Fig. 2. Surface water (5 m) data for the Canary Basin showing (a) salinity, (b) temperature, (c) nitrate (open squares) and phosphate (grey circles) and (d) DFe, against distance from the North West African coast.

elsewhere (Sarthou et al., 2007). Generally, the aerosol fluxes were low for this region at the time of the cruise. The highest fluxes occurred at the beginning of the cruise (5–8th October) in the north of the study region with soluble iron fluxes to the surface ocean ranging between 180 and 673 nmol m^{-2} d^{-1}. The flux decreased significantly following this period and the range was <0.7–22 nmol m^{-2} d^{-1} for the remainder of the cruise. Satellite imagery also showed a decrease in monthly average aerosol optical depths following the summer months (July–October 2002) obtained by the MODIS satellite (http://modis-atmos.gsfc.nasa.gov).

3.2. Spatial distribution of dissolved iron species and major nutrients in surface waters

Nitrate concentrations in the surface waters (Fig. 2(c)) were very low and varied from below the limit of detection of the spectro-photometric method (10 nM) to 80 nM, suggesting that surface waters of the entire region were depleted in nitrate. Phosphate concentrations (Fig. 2(c)) were also low, existing between the limit of detection (9 nM) and 100 nM with the highest values near the coast. Surface DFe concentrations (Fig. 2(d)) varied between 0.15 and 0.95 nM over the sampling grid and the range of data compared well with those of 'shipboard' DFe determined using another FI-CL method (0.16–0.76 nM (Sarthou et al., 2007)), and a study covering the region in October 2000 (0.2–1.2 nM (Sarthou et al., 2003)). Lower and less variable DFe concentrations were observed in the northern and western transects, which were the furthest away from the North West African continental margin. The highest concentrations (0.50–0.95 nM) were found in the south eastern corner of the grid near to the shelf and coastal upwelling region.

The negative relationship between surface DFe and the distance from the North West African coast illustrates the role of the continental shelf as a source of iron for this area. The relationship was dissimilar to the spatial distribution of DAl, which is indicative of aerosol deposition and has a longer surface water residence time (3–4 years, Orians and Bruland, 1985) compared with Fe (3 weeks–5 months; Sarthou et al., 2003; Bergquist and Boyle, 2006). In contrast to DFe, DAl concentrations were highest in the furthest stations from the coast (Kramer et al., 2004) and it was concluded that a continental source of waters rich in Fe but not Al was influencing the DFe distribution (Sarthou et al., 2007). Hence, the overall advection of shelf and upwelled waters was considered to be the dominant source of DFe to this region in the months leading up to the cruise.

3.3. Vertical distributions of size fractionated Fe species compared with other variables in the upper water column

DFe, SFe and CFe were determined for all vertical profiles (Table 1) and plots of vertical distributions of iron species, along with cell counts, chlorophyll, nutrient and physical data are shown in Figs. 3 and 4. Generally, the maximum Chl a concentrations and cell population counts were observed at the top of the nutricline and below the surface mixed layer at the hydrocast stations. At similar depths to the Chl a and cell count maxima, a nitrite maximum was observed which was used as a proxy for microbial activity. Chl a concentrations were low throughout the region (mean 0.13 ± 0.08 μg L^{-1}, 0–150 m). Exceptions were at casts 18 and 20, near the North West African shelf, where concentrations exceeded 0.25 μg L^{-1} at the deep chlorophyll maximum (DCM). The taxonomy of the phytoplankton was dominated by small picoplankton (<2 μm), specifically *Prochlorococcus* spp., *Synechococcus* spp. and two groups of picoeukaryotes (Gerringa et al., 2004). The cell number maximum ranged between 20 and 60,000 cells mL^{-1} and generally occurred within 30 m of the chlorophyll maximum.

DFe concentrations in the depth profiles ranged between 0.1 and 1.0 nM with a mean concentration of 0.42 ± 0.03 nM (n = 71) for the study area. The DFe concentrations were consistently lower than the iron binding ligand concentrations, which ranged between 0.5 and 5 nM with a mean of 1.79 nM (n = 47) (Gerringa et al., 2006). The minimum shipboard DFe concentrations in the profiles reported by Sarthou et al. (2007) typically coincided with the Chl a maximum, indicating that DFe concentrations in the DCM were influenced by biological uptake and/or controlled by interactions with particles. However, there was generally no consistent vertical trend in DFe in the upper water column (<200 m) when all the profiles were compared. This can be explained, for the most part, by spatial variation in sources and sinks of iron in the region. Examples include (i) the low and sporadic dust deposition fluxes, (ii) iron supply by mixing and advection of shelf and upwelled waters and (iii) varying uptake efficiencies of populations of phytoplankton.

Table 1
Size fractionated DFe data for all vertical profiles in the Canary Basin, sampled in October 2002. The standard deviations of analytical replicates are shown in brackets for each measurement. The estimated uncertainty for CFe (also in brackets) is the sum of the standard deviations of both DFe and SFe. Dashes (−) indicate samples that were contaminated.

Cast station	Depth (m)	DFe (nM)	SFe (nM)	CFe (nM)
8 (08/10/2002) 31.71°N, 20.00°W	2	0.45 (0.02)	0.28 (0.03)	0.17 (0.05)
	25	0.58 (0.06)	0.39 (0.04)	0.18 (0.10)
	100	0.33 (0.03)	0.35 (0.08)	0.00 (0.12)
	150	0.49 (0.03)	0.52 (0.07)	−0.03 (0.10)
10 (09/10/2002) 31.71°N, 22.00°W	25	0.31 (0.02)	0.14 (0.01)	0.17 (0.03)
	50	0.31 (0.03)	0.17 (0.02)	0.14 (0.04)
	70	0.37 (0.05)	0.15 (0.02)	0.22 (0.07)
	100	0.33 (0.05)	0.26 (0.02)	0.07 (0.07)
	125	0.40 (0.05)	0.21 (0.03)	0.19 (0.08)
	150	0.47 (0.03)	0.22 (0.02)	0.25 (0.05)
	600	0.44 (0.04)	0.27 (0.03)	0.17 (0.07)
	1300	0.54 (0.04)	0.32 (0.05)	0.22 (0.09)
11 (10/10/2002) 31.71°N, 24.00°W	25	0.30 (0.03)	0.15 (0.01)	0.14 (0.04)
	50	0.18 (0.01)	0.15 (0.02)	0.03 (0.04)
	70	0.27 (0.03)	0.19 (0.02)	0.09 (0.06)
	80	0.58 (0.02)	0.13 (0.03)	0.45 (0.05)
	100	0.40 (0.03)	0.18 (0.02)	0.22 (0.05)
	150	0.37 (0.04)	0.16 (0.02)	0.21 (0.06)
13 (11/10/2002) 29.62°N, 23.98°W	25	0.44 (0.02)	0.14 (0.02)	0.30 (0.04)
	50	0.38 (0.03)	0.14 (0.02)	0.24 (0.06)
	70	0.42 (0.03)	0.10 (0.01)	0.32 (0.04)
	100	0.39 (0.06)	0.16 (0.03)	0.23 (0.08)
	125	0.33 (0.02)	0.13 (0.01)	0.20 (0.03)
	150	0.42 (0.03)	0.20 (0.01)	0.22 (0.03)
15 (12/10/2002) 26.78°N, 24.00°W	2	0.30 (0.02)	0.11 (0.02)	0.18 (0.04)
	25	0.82 (0.07)	0.16 (0.01)	0.65 (0.07)
	50	0.39 (0.02)	0.14 (0.01)	0.26 (0.03)
	100	0.20 (0.01)	0.26 (0.01)	−0.05 (0.03)
	125	0.39 (0.02)	0.44 (0.01)	−0.05 (0.04)
	150	0.49 (0.03)	0.41 (0.04)	0.08 (0.07)
16 (13/10/2002) 25.00°N, 24.00°W	2	0.33 (0.02)	0.34 (0.02)	−0.01 (0.04)
	25	0.31 (0.03)	−	−
	70	0.54 (0.02)	−	−
	100	0.31 (0.03)	−	−
	150	0.88 (0.04)	0.47 (0.03)	0.41 (0.07)
18 (14/10/2002) 25.00°N, 21.37°W	25	0.62 (0.04)	0.24 (0.03)	0.38 (0.07)
	50	0.54 (0.03)	0.16 (0.03)	0.38 (0.06)
	70	0.64 (0.05)	0.19 (0.02)	0.45 (0.07)
	100	0.27 (0.03)	0.19 (0.02)	0.09 (0.05)
	125	0.35 (0.06)	0.20 (0.01)	0.15 (0.07)
	150	0.49 (0.04)	0.31 (0.02)	0.18 (0.06)
20 (15/10/2002) 25.00°N, 18.86°W	2	0.63 (0.06)	0.18 (0.01)	0.45 (0.07)
	25	0.46 (0.03)	0.17 (0.03)	0.29 (0.06)
	50	0.46 (0.02)	0.27 (0.03)	0.19 (0.05)
	70	0.54 (0.03)	0.49 (0.05)	0.04 (0.08)
	100	0.73 (0.03)	0.35 (0.03)	0.38 (0.06)
	125	0.56 (0.03)	0.17 (0.03)	0.38 (0.06)
	150	0.78 (0.05)	0.29 (0.03)	0.49 (0.08)
22 (16/10/2002) 26.70°N, 19.99°W	2	0.72 (0.06)	0.44 (0.05)	0.28 (0.12)
	25	0.83 (0.05)	0.28 (0.01)	0.55 (0.06)
	50	0.51 (0.05)	0.48 (0.03)	0.03 (0.09)
	70	0.59 (0.01)	0.20 (0.01)	0.38 (0.02)
	100	0.53 (0.03)	0.32 (0.07)	0.21 (0.11)
	150	0.53 (0.02)	0.33 (0.03)	0.20 (0.05)
23 (17/10/2002) 29.25°N, 20.03°W	25	0.31 (0.03)	0.23 (0.03)	0.08 (0.06)
	50	0.33 (0.01)	0.32 (0.03)	0.00 (0.04)
	70	0.61 (0.03)	0.35 (0.03)	0.26 (0.06)
	90	0.21 (0.04)	0.22 (0.03)	−0.01 (0.06)
	100	0.25 (0.02)	0.19 (0.02)	0.06 (0.03)
	125	0.45 (0.02)	0.44 (0.03)	0.01 (0.05)
	150	0.45 (0.02)	0.20 (0.01)	0.25 (0.03)

Soluble and colloidal iron concentrations in the upper water column both varied between 0.05 and 0.7 nM. The variability of the two size fractions with depth was greatest at stations nearer the continental shelf (Fig. 3) with % CFe (i.e. (CFe/DFe) × 100%) showing standard deviations of 24.1%, 23.7% and 30.9% at casts 18, 20 and 23, respectively. The considerable vertical changes in ratios of the iron species in these near-shelf profiles support previous observations of dynamic cycling between dissolved and particulate Fe fractions in shelf waters, using stable isotope tracers in shipboard incubations (Hurst and Bruland, 2007). There are several possible explanations for the vertical changes observed here. These include the effects of biological processing and aggregation (biological control), vertical changes in concentrations and speciation of colloidal matter due to poor vertical mixing (physical control), vertical changes in chemical processes (e.g. redox cycling) and the distribution of strong Fe binding ligands in the soluble and colloidal phase (chemical partitioning).

There is strong evidence that organic Fe-ligand speciation can change due to photochemical transformations such as photoreduction of Fe-siderophore complexes (Barbeau, 2006 and references therein). Hence, photochemistry may play a role in the partitioning between SFe and CFe. However, the intensity of surface solar irradiance and the penetration of light through the upper water column at these stations would have been similar due to their close proximity. Hence this was unlikely to be the main cause of the variability observed between these different vertical profiles.

Cullen et al. (2006) examined equilibrium partitioning of iron between soluble and colloidal ligands in Atlantic samples and showed that a large proportion of colloidal iron binding sites were 'inert' to Fe exchange whereas the low molecular weight SFe was sufficiently labile to exchange between size fractions. Therefore control by chemical exchange between the two size fractions would not explain the significant vertical gradients seen in CFe at these near-shelf stations.

In some cases, vertical changes in colloids and Fe speciation occurred alongside the mixing gradients of different water masses. This is best illustrated in cast 18 (Fig. 3) where a significant shift in iron size speciation was observed between the mixed layer and the seasonal thermocline. The vertical profile of organic speciation data reported for this station (Gerringa et al., 2006) showed decreasing dissolved Fe-ligand concentrations (L) from 3.96 nM, at 10 m to 0.83 nM, at 150 m. However, no major change in L occurred between the transition between the base of the mixed layer (25–60 m) and the top of the thermocline (ca. 80–100 m), reaffirming that Fe binding ligand concentration was not controlling Fe size speciation.

Interestingly, CFe concentration minima often coincided with the nitrite maximum (near to the DCM and cell population maxima) suggesting that biological activity was either affecting or being affected by the dissolved iron size speciation at these depths. Minima for CFe were also observed between 30 and 80 m in the central North Atlantic gyre (Bergquist et al., 2007) suggesting that this is a common phenomenon. Possible explanations for this observation include the transformation of CFe into larger particles (e.g. aggregation with cells and particles) or biological processing of colloids (e.g. production of SFe or bioavailable Fe). Indeed, biological uptake or breakdown of Fe associated with colloidal matter may have occurred as Fe associated with biogenic and inorganic colloids can be bioavailable to certain species (Chen et al., 2003; Nodwell and Price, 2001).

In contrast to the stations nearer the shelf, the fractionation at the most remote, less productive stations (Fig. 4) was less variable throughout the upper water column. The % CFe fraction for the vertical profiles had standard deviations of 13.7%, 16.1% and 8.0%, for casts 10, 11 and 13, respectively. This suggests the iron size
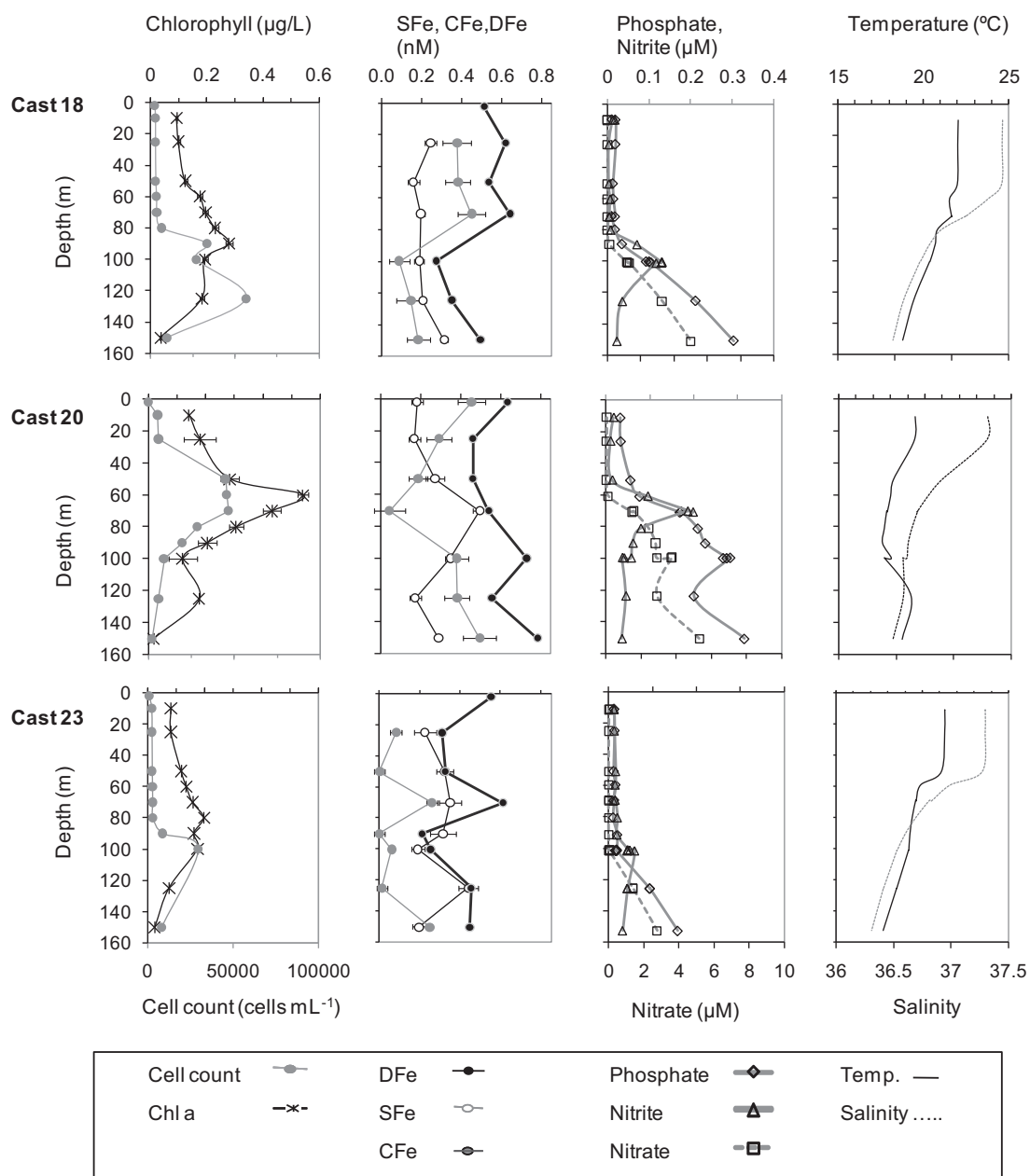
Fig. 3. Vertical distributions of size fractionated iron and physico-chemical parameters in the upper water column of the Canary Basin, near the North West African shelf.

speciation at these oligotrophic stations was less influenced by the microbial community and mixing, and that the vertical distributions of SFe and CFe were influenced more by chemical equilibrium between soluble, colloidal and particulate phases.

This is supported by data from intermediate waters from a deep cast (cast 10 at 31.7°N, 22.0°W) (Fig. 5). At this station, CFe concentrations constituted a major fraction of DFe (ca. 25–60%) in these waters, consistent with the high percentage of CFe observed in the DFe pool in the Northeast Pacific and North Atlantic Oceans (e.g. 13–50%, 200–600 m (Nishioka et al., 2001) and 30–70%, 200–6000 m (Wu et al., 2001)). The intermediate waters in this area were influenced by intrusion of high salinity Mediterranean Outflow Water (MOW, 600–1500 m, salinity = 35.6, temperature 7–10 °C), which coincided with nitrate, phosphate and silicate maxima. Within these waters, % CFe was relatively consistent between 600 and 1300 m (38% and 41%, respectively) suggesting

a steady-state between colloidal and soluble forms of Fe had been reached within this older water mass.

The data for cast 10 also showed that DFe increased from 0.3 to 0.4 nM in the surface waters (0–150 m) to 0.5–0.6 nM in deep waters. Determination of SFe and CFe size fractions showed that the depletion of DFe in the surface water coincided with low SFe concentrations which more than doubled with depth (0.14 nM at the surface to 0.32 nM at 1300 m). This was consistent with the concentration gradient for SFe reported by Wu et al. (2001) for two stations in the North Atlantic (22.8°N, 36.8°W and 34.8°N, 57.8°W). In this case, the depleted soluble iron concentrations in the surface waters of cast 10 may reflect some preference of phytoplankton and bacteria in this oligotrophic region for the SFe fraction, as the most significant change with depth was observed at the base of the upper water column (100–200 m) below the euphotic zone.
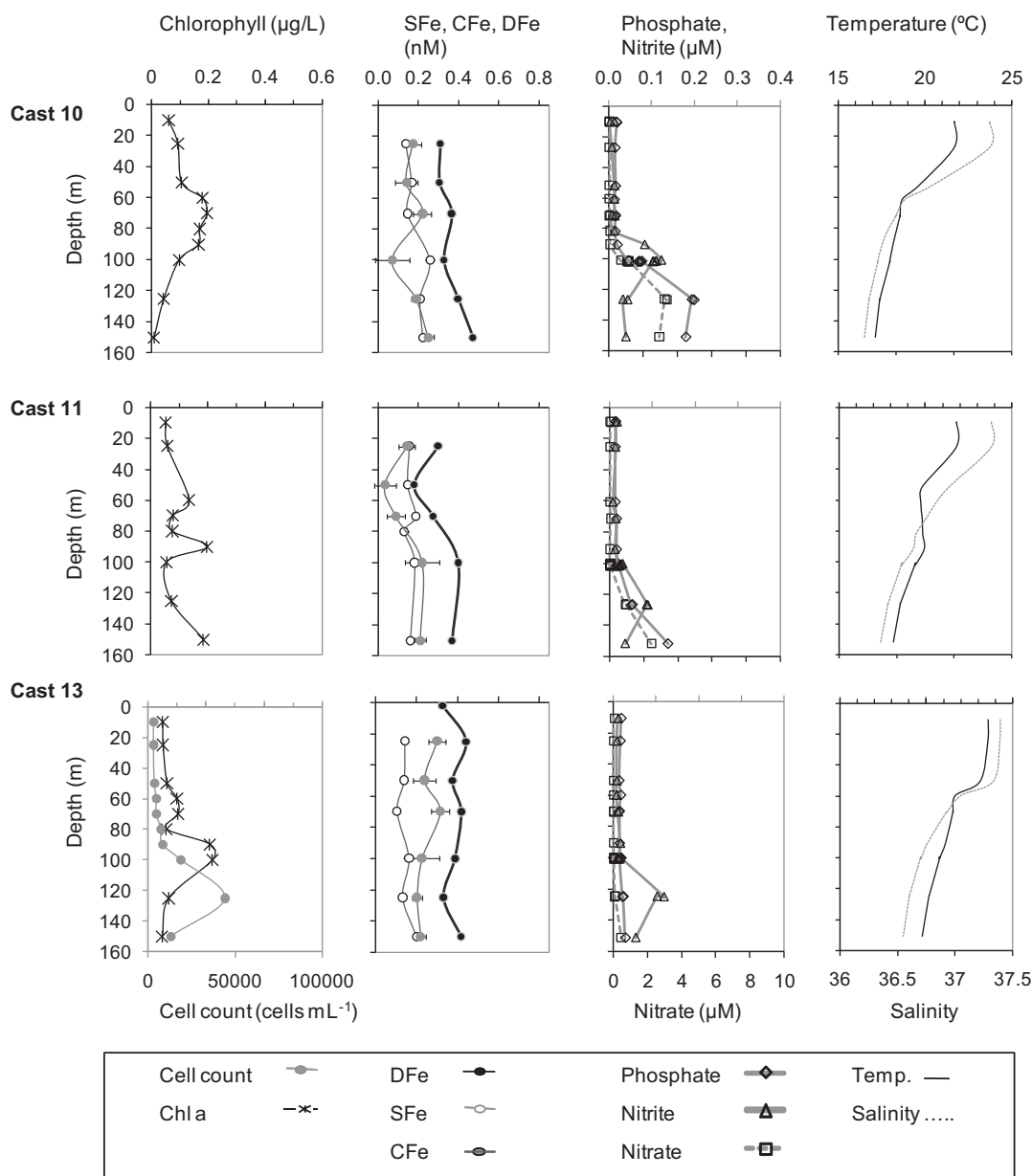
Fig. 4. Vertical distributions of size fractionated iron and physico-chemical parameters in the upper water column of the most remote stations in the Canary Basin.

Although no iron binding ligand data were available for cast 10, another explanation for the observed SFe profile is that soluble Fe-ligand concentrations were depleted in surface waters due to photo-degradation and uptake, and enhanced at depth following regeneration below the euphotic zone. This explanation is more consistent with the conclusion that vertical changes in Fe binding ligands control vertical changes in Fe solubility in the open ocean. Strong evidence for ligands/seawater composition controlling SFe has been presented (Kuma et al., 1998, 1996; Tani et al., 2003) where significant variability in the solubility of Fe with depth was observed in seawaters amended with high iron concentrations (100 nM).

The possibility of a relationship of SFe and CFe with particulate associated Fe was also examined using cast 10 data. Sarthou et al. (2007) showed considerable variability in particulate Fe (>0.2 μm) in this region with significantly higher concentrations found in the near-surface waters (0–25 m) and intermediate/deep waters (200–4000 m) with low concentrations between 50 and 150 m. Hence, SFe and CFe concentrations appear not to be closely linked to *in situ* particulate Fe concentrations, especially in the more dynamic surface waters.

3.4. Variability in soluble and colloidal Fe concentrations over the Canary Basin

Overall, both SFe and CFe fractions formed a significant percentage of DFe in the Canary Basin and the mean % CFe ($\pm$sd) was 42 ($\pm$24) %. The variation in soluble and colloidal iron concentrations of all the data is shown in a histogram (Fig. 6). Both fractions showed a skewed distribution towards lower concentrations (0–0.3 nM) with mean values of 0.25 and 0.21 nM, for SFe and CFe, respectively ($n = 58$). The CFe fraction is likely to include Fe from aerosol fluxes to surface waters and recycled iron incorporated in organic matter. Nishioka et al. (2001) reported much lower concentrations of colloidal Fe (200 kDa–0.2 μm) in the mixed layer of the remote Northeast Pacific waters (0.01–0.06 nM). However, Wu et al. (2001) observed higher and more variable concentrations
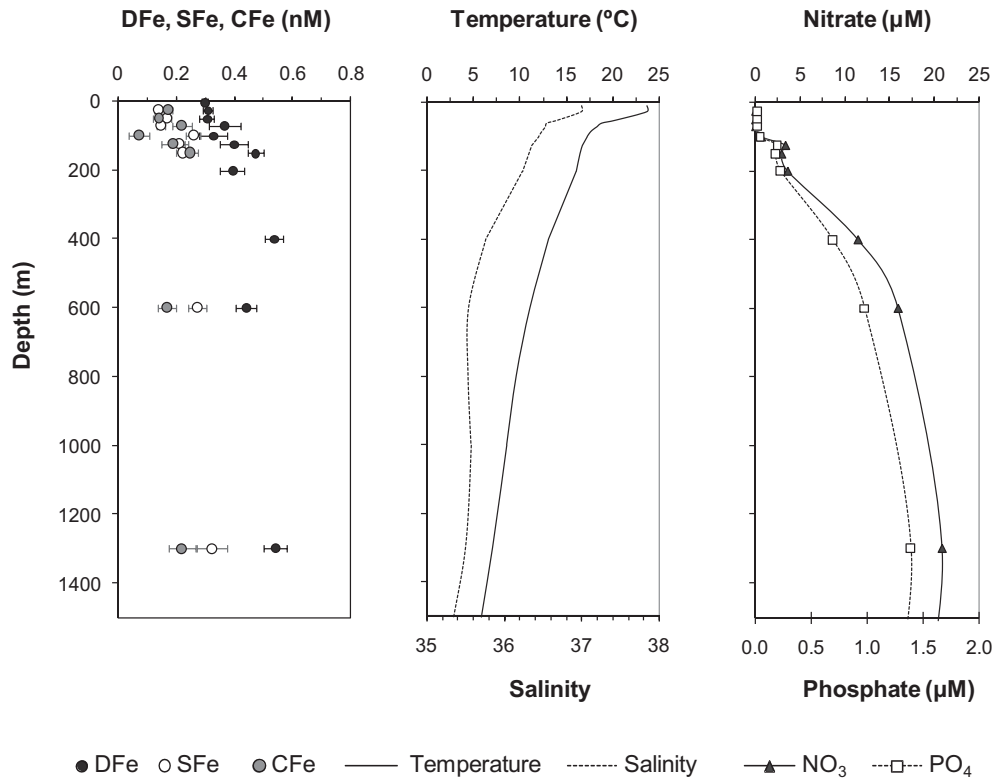
Fig. 5. Dissolved iron (DFe) size speciation and physico-chemical data for surface and intermediate waters at cast station 10 (31.7°N, 22.0°W).

(0.1–0.8 nM) in the water column for two stations in the North Atlantic Ocean (22.8°N, 36.8°W, September 1999, 34.8°N, 57.8°W, July 1998) and a station in the North Pacific near Hawaii (22.8°N, 158.8°W).

To test whether the negative trend in DFe with distance from the coast (discussed in Section 3.2) was a result of changes in either CFe or SFe, all of the cast size speciation data was integrated between 0 and 150 m depth (using trapezoid integration and assuming
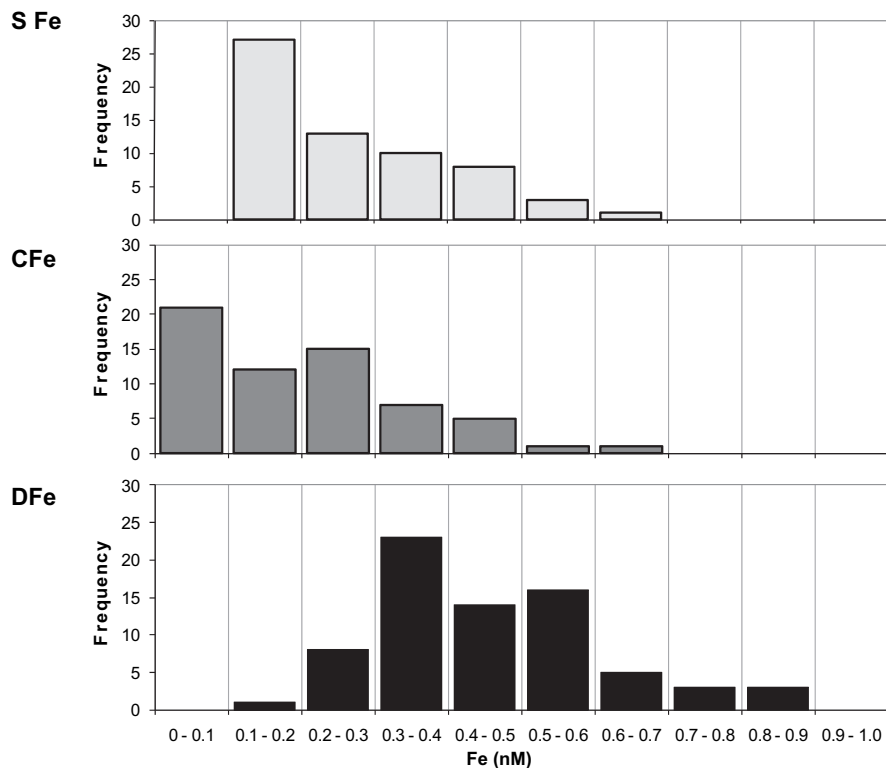

Fig. 6. Histograms showing the frequency distribution of size fractionated dissolved iron (DFe) species in the euphotic zone of the Canary Basin study area.
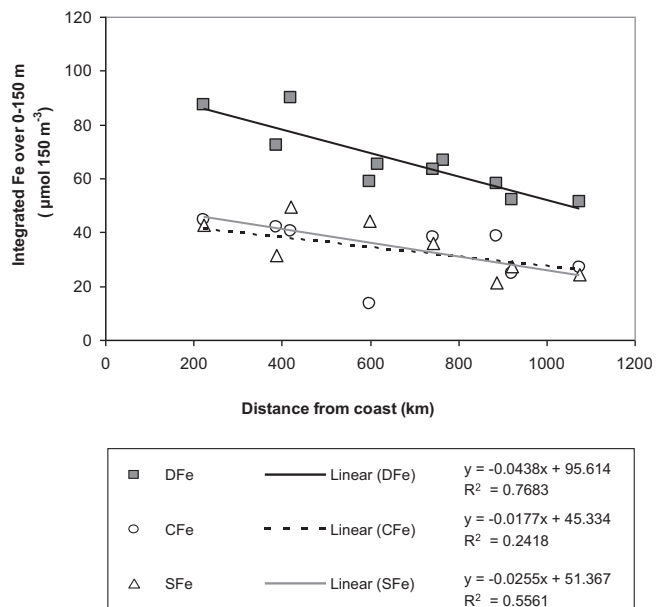
Fig. 7. Relationship between integrated concentrations of DFe, CFe and SFe from casts (0–150 m) and distance from the North West African coast.

a 1 m^2 column of water). The data showed considerable scatter but the linear trends showed that the concentration of both CFe and SFe species decreased with distance from the North West African coastline (Fig. 7). This is interesting as it is in contrast to the observation of the horizontal variability of surface open ocean DFe being predominantly related to variability in CFe (Bergquist et al., 2007). It also provides evidence that SFe can vary significantly between water masses depending on physico-chemical variables and the composition of the water.

4. Conclusions

A trend of decreasing DFe with distance from the North West African shelf in the upper water column of the Canary Basin was observed in October 2002, with no evidence of any large scale dust deposition during or prior to the study. The study showed that the trend was caused by decreasing concentrations in both SFe and CFe, and each formed a significant proportion of DFe (mean values of 0.25 and 0.21 nM, respectively) when the whole study area was considered. Greater vertical variability in both fractions was observed in the stations nearest the shelf and physico-chemical and flow cytometry data indicated that mixing and biological processes were controlling vertical changes in Fe size fractionation between SFe and CFe in this region. Further northwest, approaching the remote waters of the North Atlantic gyre, less variability in the vertical size fractionation of Fe was observed. This suggests that these waters were closer to a steady-state with respect to iron partitioning between dissolved size fractions.

Acknowledgements

References

Baker, A.R., Jickells, T.D., Witt, M., Linge, K.L., 2006. Trends in the solubility of iron, aluminium, manganese and phosphorus in aerosol collected over the Atlantic Ocean. Marine Chemistry 98 (1), 43–58.

Barbeau, K., 2006. Photochemistry of organic iron(III) complexing ligands in oceanic systems. Photochemistry and Photobiology 82, 1505–1516.

Barton, E.D., 1998. The global coastal ocean: regional studies and syntheses. In: Robinson, A., Bri, K. (Eds.), The Sea. Wiley, New York.

Bergquist, B.A., Boyle, E.A., 2006. Dissolved iron in the tropical and subtropical Atlantic Ocean. Global Biogeochemical Cycles 20, GB1015. doi:10.1029/2005GB002505.

Bergquist, B.A., Wu, J., Boyle, E.A., 2007. Variability in oceanic dissolved iron is dominated by the colloidal fraction. Geochimica et Cosmochimica Acta 71 (12), 2960–2974.

Blain, S., Sarthou, G., Laan, P., 2008. Distribution of dissolved iron during the natural iron-fertilization experiment KEOPS (Kerguelen Plateau, Southern Ocean). Deep-Sea Research Part II – Topical Studies in Oceanography 55, 594–605.

Bowie, A.R., Achterberg, E.P., Croot, P.L., de Baar, H.J.W., Laan, P., Moffett, J.W., Ussher, S., Worsfold, P.J., 2006. A community-wide intercomparison exercise for the determination of dissolved iron in seawater. Marine Chemistry 98 (1), 81–99.

Bowie, A.R., Achterberg, E.P., Mantoura, R.F.C., Worsfold, P.J., 1998. Determination of sub-nanomolar levels of iron in seawater using flow injection with chemiluminescence detection. Analytica Chimica Acta 361 (3), 189–200.

Bowie, A.R., Ussher, S.J., Landing, W.M., Worsfold, P.J., 2007. Intercomparison between FI-CL and ICP-MS for the determination of dissolved iron in Atlantic seawater. Environmental Chemistry 4 (1), 1–4.

Boyd, P.W., Watson, A.J., Law, C.S., Abraham, E.R., Trull, T., Murdoch, R., Bakker, D.C. E., Bowie, A.R., Buesseler, K.O., Chang, H., Charette, M., Croot, P., Downing, K., Frew, R., Gall, M., Hadfield, M., Hall, J., Harvey, M., Jameson, G., LaRoche, J., Liddicoat, M., Ling, R., Maldonado, M.T., McKay, R.M., Nodder, S., Pickmere, S., Pridmore, R., Rintoul, S., Safi, K., Sutton, P., Strzepek, R., Tanneberger, K., Turner, S., Waite, A., Zeldis, J., 2000. A mesoscale phytoplankton bloom in the polar Southern Ocean stimulated by iron fertilization. Nature 407 (6805), 695–702.

Bruland, K.W., Orians, K.J., Cowen, J.P., 1994. Reactive trace-metals in the stratified central North Pacific. Geochimica et Cosmochimica Acta 58 (15), 3171–3182.

Buck, C.S., Landing, W.M., Resing, J.A., Lebon, G.T., 2006. Aerosol iron and aluminum solubility in the northwest Pacific Ocean: results from the 2002 IOC cruise. Geochemistry Geophysics Geosystems 7.

Byrne, R.H., Luo, Y.R., Young, R.W., 2000. Iron hydrolysis and solubility revisited: observations and comments on iron hydrolysis characterizations. Marine Chemistry 70 (1–3), 23–35.

Chase, Z., Johnson, K.S., Elrod, V.A., Plant, J.N., Fitzwater, S.E., Pickell, L., Sakamoto, C. M., 2005. Manganese and iron distributions off central California influenced by upwelling and shelf width. Marine Chemistry 95 (3–4), 235–254.

Chen, M., Dei, R.C.H., Wang, W.X., Guo, L.D., 2003. Marine diatom uptake of iron bound with natural colloids of different origins. Marine Chemistry 81 (3–4), 177–189.

Coale, K.H., Johnson, K.S., Chavez, F.P., Buesseler, K.O., Barber, R.T., Brzezinski, M.A., Cochlan, W.P., Millero, F.J., Falkowski, P.G., Bauer, J.E., Wanninkhof, R.H., Kudela, R.M., Altabet, M.A., Hales, B.E., Takahashi, T., Landry, M.R., Bidigare, R.R., Wang, X.J., Chase, Z., Strutton, P.G., Friederich, G.E., Gorbunov, M.Y., Lance, V.P., Hilting, A.K., Hiscock, M.R., Demarest, M., Hiscock, W.T., Sullivan, K.F., Tanner, S. J., Gordon, R.M., Hunter, C.N., Elrod, V.A., Fitzwater, S.E., Jones, J.L., Tozzi, S., Koblizek, M., Roberts, A.E., Herndon, J., Brewster, J., Ladizinsky, N., Smith, G., Cooper, D., Timothy, D., Brown, S.L., Selph, K.E., Sheridan, C.C., Twining, B.S., Johnson, Z.I., 2004. Southern ocean iron enrichment experiment: carbon cycling in high- and low-Si waters. Science 304 (5669), 408–414.

Coale, K.H., Johnson, K.S., Fitzwater, S.E., Gordon, R.M., Tanner, S., Chavez, F.P., Ferioli, L., Sakamoto, C., Rogers, P., Millero, F., Steinberg, P., Nightingale, P., Cooper, D., Cochlan, W.P., Landry, M.R., Constantinou, J., Rollwagen, G., Trasvina, A., Kudela, R., 1996. A massive phytoplankton bloom induced by an ecosystem-scale iron fertilization experiment in the equatorial Pacific Ocean. Nature 383 (6600), 495–501.

Croot, P.L., Laan, P., 2002. Continuous shipboard determination of Fe(II) in polar waters using flow injection analysis with chemiluminescence detection. Analytica Chimica Acta 466 (2), 261–273.

Cullen, J.T., Bergquist, B.A., Moffett, J.W., 2006. Thermodynamic characterization of the partitioning of iron between soluble and colloidal species in the Atlantic Ocean. Marine Chemistry 98 (2–4), 295–303.

de Baar, H.J.W., de Jong, J.T.M., 2001. Distributions, sources and sinks of iron in seawater. In: Hunter, K.A., Turner, D.R. (Eds.), The Biogeochemistry of Iron in Seawater. John Wiley, New York, pp. 123–153.

de Jong, J.T.M., den Das, J., Bathmann, U., Stoll, M.H.C., Kattner, G., Nolting, R.F., de Baar, H.J.W., 1998. Dissolved iron at subnanomolar levels in the Southern Ocean as determined by ship-board analysis. Analytica Chimica Acta 377 (2–3), 113–124.

Duce, R.A., Tindale, N.W., 1991. Atmospheric transport of iron and its deposition in the ocean. Limnology and Oceanography 36 (8), 1715–1726.

Elrod, V.A., Berelson, W.M., Coale, K.H., Johnson, K.S., 2004. The flux of iron from continental shelf sediments: a missing source for global budgets. Geophysical Research Letters 31 (12) art. no. L12307.

Falkowski, P.G., Barber, R.T., Smetacek, V., 1998. Biogeochemical controls and feedbacks on ocean primary production. Science 281 (5374), 200–206.

Gerringa, L.J.A., Rijkenberg, M.J.A., Timmermans, K.R., Buma, A.G.J., 2004. The influence of solar ultraviolet radiation on the photochemical production of H_2O_2 in the equatorial Atlantic Ocean. Journal of Sea Research 51 (1), 3–10.

Gerringa, L.J.A., Veldhuis, M.J.W., Timmermans, K.R., Sarthou, G., de Baar, H.J.W., 2006. Co-variance of dissolved Fe-binding ligands with phytoplankton characteristics in the Canary Basin. Marine Chemistry 102 (3–4), 276–290.

Grashoff, K., Erhardt, M., Kremling, K., 1983. Methods of Seawater Analysis. Wiley-Vch.

Hurst, M.P., Bruland, K.W., 2007. An investigation into the exchange of iron and zinc between soluble, colloidal, and particulate size-fractions in shelf waters using low-abundance isotopes as tracers in shipboard incubation experiments. Marine Chemistry 103 (3–4), 211–226.

Jickells, T.D., 1999. The inputs of dust derived elements to the Sargasso Sea; a synthesis. Marine Chemistry 68 (1–2), 5–14.

Jickells, T.D., An, Z.S., Andersen, K.K., Baker, A.R., Bergametti, G., Brooks, N., Cao, J.J., Boyd, P.W., Duce, R.A., Hunter, K.A., Kawahata, H., Kubilay, N., La Roche, J., Liss, P.S., Mahowald, N., Prospero, J.M., Ridgwell, A.J., Tegen, I., Torres, R., 2005. Global iron connections between desert dust, ocean biogeochemistry, and climate. Science 308 (5718), 67–71.

Johnson, K.S., Boyle, E., Bruland, K., Coale, K., Measures, C., Moffett, J., Aguilarislas, A., Barbeau, K., Bergquist, B., Bowie, A., Buck, K., Cai, Y., Chase, Z., Cullen, J., Doi, T., Elrod, V., Fitzwater, S., Gordon, M., King, A., Laan, P., Laglera-Baquer, L., Landing, W., Lohan, M., Mendez, J., Milne, A., Obata, H., Ossiander, L., Plant, J., Sarthou, G., Sedwick, P., Smith, G.J., Sohst, B., Tanner, S., Van den Berg, S., Wu, J., 2007. Developing standards for dissolved iron in seawater. EOS, Transactions, American Geophysical Union 88 (11), 131–132.

Johnson, W.K., Miller, L.A., Sutherland, N.E., Wong, C.S., 2005. Iron transport by mesoscale Haida eddies in the Gulf of Alaska. Deep-Sea Research Part II – Topical Studies in Oceanography 52 (7–8), 933–953.

Kramer, J., Laan, P., Sarthou, G., Timmermans, K.R., de Baar, H.J.W., 2004. Distribution of dissolved aluminium in the high atmospheric input region of the subtropical waters of the North Atlantic Ocean. Marine Chemistry 88 (3–4), 85–101.

Kremling, K., Streu, P., 1993. Saharan dust influenced trace-element fluxes in deep North-Atlantic subtropical waters. Deep-Sea Research Part I – Oceanographic Research Papers 40 (6), 1155–1168.

Kuma, K., Katsumoto, A., Kawakami, H., Takatori, F., Matsunaga, K., 1998. Spatial variability of Fe(III) hydroxide solubility in the water column of the northern North Pacific Ocean. Deep-Sea Research Part I – Oceanographic Research Papers 45 (1), 91–113.

Kuma, K., Nishioka, J., Matsunaga, K., 1996. Controls on iron(III) hydroxide solubility in seawater: the influence of pH and natural organic chelators. Limnology and Oceanography 41 (3), 396–407.

Kuss, J., Kremling, K., 1999a. Particulate trace element fluxes in the deep northeast Atlantic Ocean. Deep-Sea Research Part I – Oceanographic Research Papers 46 (1), 149–169.

Kuss, J., Kremling, K., 1999b. Spatial variability of particle associated trace elements in near-surface waters of the North Atlantic (30 degrees N/60 degrees W to 60 degrees N/2 degrees W), derived by large-volume sampling. Marine Chemistry 68 (1–2), 71–86.

Lam, P.J., Bishop, J.K.B., Henning, C.C., Marcus, M.A., Waychunas, G.A., Fung, I.Y., 2006. Wintertime phytoplankton bloom in the subarctic Pacific supported by continental margin iron. Global Biogeochemical Cycles 20 (1), GB1006. doi:10.1029/2005GB002557.

Landing, W.M., Bruland, K.W., 1987. The contrasting biogeochemistry of iron and manganese in the Pacific Ocean. Geochimica et Cosmochimica Acta 51 (1), 29–43.

Liu, X.W., Millero, F.J., 1999. The solubility of iron hydroxide in sodium chloride solutions. Geochimica et Cosmochimica Acta 63 (19–20), 3487–3497.

Liu, X.W., Millero, F.J., 2002. The solubility of iron in seawater. Marine Chemistry 77 (1), 43–54.

Martin, J.H., Coale, K.H., Johnson, K.S., Fitzwater, S.E., Gordon, R.M., Tanner, S.J., Hunter, C.N., Elrod, V.A., Nowicki, J.L., Coley, T.L., Barber, R.T., Lindley, S., Watson, A.J., Van Scoy, K., Law, C.S., Liddicoat, M.I., Ling, R., Stanton, T., Stockel, J., 1994. Testing the iron hypothesis in ecosystems of the equatorial Pacific Ocean. Nature 371 (6493), 123–129.

Martin, J.H., Fitzwater, S.E., 1988. Iron-deficiency limits phytoplankton growth in the northeast Pacific subarctic. Nature 331 (6154), 341–343.

Nishioka, J., Takeda, S., Wong, C.S., Johnson, W.K., 2001. Size-fractionated iron concentrations in the northeast Pacific Ocean: distribution of soluble and small colloidal iron. Marine Chemistry 74 (2–3), 157–179.

Nodwell, L.M., Price, N.M., 2001. Direct use of inorganic colloidal iron by marine mixotrophic phytoplankton. Limnology and Oceanography 46 (4), 765–777.

Orians, K.J., Bruland, K.W., 1985. Dissolved aluminum in the Central North Pacific. Nature 316 (6027), 427–429.

Pelegrí, J.L., Arístegui, J., Cana, L., González-Dávila, M., Hernández-Guerra, A., Hernández-León, S., Marrero-Díaz, A., Montero, M.F., Sangrà, P., Santana-Casiano, M., 2005. Coupling between the open ocean and the coastal upwelling region off northwest Africa: water recirculation and offshore pumping of organic matter. Journal of Marine Systems 54 (1–4), 3–37.

Planquette, H., Statham, P.J., Fones, G.R., Charette, M.A., Moore, C.M.M., Salter, I., Nédélec, F.H., Taylor, S.L., French, M., Baker, A.R., Mahowald, N., Jickells, T.D., 2007. Dissolved iron in the vicinity of the Crozet Islands, Southern Ocean. Deep-Sea Research Part II – Topical Studies in Oceanography 54, 1999–2019.

Planquette, H., Fones, G.R., Statham, P.J., Morris, P.J., 2009. Origin of iron and aluminium in large particles (>53 μm) in the Crozet region, Southern Ocean. Marine Chemistry 115, 31–42.

Powell, R.T., Donat, J.R., 2001. Organic complexation and speciation of iron in the South and Equatorial Atlantic. Deep-Sea Research Part II – Topical Studies in Oceanography 48 (13), 2877–2893.

Rue, E.L., Bruland, K.W., 1995. Complexation of Iron(III) by natural organic-ligands in the central North Pacific as determined by a new competitive ligand equilibration adsorptive cathodic stripping voltammetric method. Marine Chemistry 50 (1–4), 117–138.

Sarthou, G., Baker, A.R., Blain, S., Achterberg, E.P., Boye, M., Bowie, A.R., Croot, P., Laan, P., de Baar, H.J.W., Jickells, T.D., Worsfold, P.J., 2003. Atmospheric iron deposition and sea-surface dissolved iron concentrations in the eastern Atlantic Ocean. Deep-Sea Research Part I – Oceanographic Research Papers 50 (10–11), 1339–1352.

Sarthou, G., Baker, A.R., Kramer, J., Laan, P., Laes, A., Ussher, S., Achterberg, E.P., de Baar, H.J.W., Timmermans, K.R., Blain, S., 2007. Influence of atmospheric inputs on the iron distribution in the subtropical North-East Atlantic Ocean. Marine Chemistry 104 (3–4), 186–202.

Sedwick, P.N., Church, T.M., Bowie, A.R., Marsay, C.M., Ussher, S.J., Achilles, K.M., Lethaby, P.J., Johnson, R.J., Sarin, M.M., McGillicuddy, D.J., 2005. Iron in the Sargasso Sea (Bermuda Atlantic Time-series Study region) during summer: Eolian imprint, spatiotemporal variability, and ecological implications. Global Biogeochemical Cycles 19 (4).

Tani, H., Nishioka, J., Kuma, K., Takata, H., Yamashita, Y., Tanoue, E., Midorikawa, T., 2003. Iron(III) hydroxide solubility and humic-type fluorescent organic matter in the deep water column of the Okhotsk Sea and the northwestern North Pacific Ocean. Deep Sea Research Part I – Oceanographic Research Papers 50 (9), 1063–1078.

Torres-Padron, M.E., Gelado-Caballero, M.D., Collado-Sanchez, C., Siruela-Matos, V. F., Cardona-Castellano, P.J., Hernandez-Brito, J.J., 2002. Variability of dust inputs to the CANIGO zone. Deep-Sea Research Part II – Topical Studies in Oceanography 49 (17), 3455–3464.

Tsuda, A., Takeda, S., Saito, H., Nishioka, J., Nojiri, Y., Kudo, I., Kiyosawa, H., Shiomoto, A., Imai, K., Ono, T., Shimamoto, A., Tsumune, D., Yoshimura, T., Aono, T., Hinuma, A., Kinugasa, M., Suzuki, K., Sohrin, Y., Noiri, Y., Tani, H., Deguchi, Y., Tsurushima, N., Ogawa, H., Fukami, K., Kuma, K., Saino, T., 2003. A mesoscale iron enrichment in the western subarctic Pacific induces a large centric diatom bloom. Science 300 (5621), 958–961.

Ussher, S.J., Achterberg, E.P., Worsfold, P.J., 2004. Marine biogeochemistry of iron. Environmental Chemistry 1 (2), 67–80.

van den Berg, C.M.G., 1995. Evidence for organic complexation of iron in seawater. Marine Chemistry 50 (1–4), 139–157.

Veldhuis, M.J.W., Kraay, G.W., 2004. Phytoplankton in the subtropical Atlantic Ocean: towards a better assessment of biomass and composition. Deep Sea Research Part I – Oceanographic Research Papers 51 (4), 507–530.

Wu, J.F., Boyle, E., Sunda, W., Wen, L.S., 2001. Soluble and colloidal iron in the oligotrophic North Atlantic and North Pacific. Science 293 (5531), 847–849.